

Supporting Information

Heterostructured Cu₂O/CuO decorated with nickel as a highly efficient photocathode for photoelectrochemical water reduction

Amare Aregahegn Dubale^{1,†}, Chun-Jern Pan^{1,†}, Andebet Gedamu Tamirat¹, Hung-Ming-Chen¹, Wei-Nien Su^{2,*}, Ching-Hsiang Chen^{2,*}, John Rckik¹, Delele Worku Ayele¹, Belete Asefa Aragaw¹, Jyh-Fu Lee³, Yaw-Wen Yang³ and Bing-Joe Hwang^{1,3*}

¹ NanoElectrochemistry Laboratory, Department of Chemical Engineering, National Taiwan University of Science and Technology, Taipei 106, Taiwan.

² NanoElectrochemistry Laboratory, Graduate Institute of Applied Science and Technology, National Taiwan University of Science and Technology, Taipei 106, Taiwan.

³ National Synchrotron Radiation Research Center, Hsinchu 30076, Taiwan.

† These authors contribute equally

* Corresponding authors: bjh@mail.ntust.edu.tw; wsu@mail.ntust.edu.tw;
bluse@mail.ntust.edu.tw

The XRD patterns of the as synthesized Cu film together with thermally oxidized copper at 350 °C in air for 0.5 to 4 hr and Cu film annealed at 350 °C to 650 °C for 4 hour are given in Figure 1(a) and Figure 4(a) respectively. As reported elsewhere, the intensity of the strongest characteristic diffraction peaks of CuO (111), Cu₂O (111) and Cu (111) planes can be used for roughly determining of the relative amount of Cu₂O phase (wt%) in the Cu₂O/CuO composite.¹ The results of relative amount of Cu₂O determined by intensity ratio $\text{Cu}_2\text{O}/[\text{Cu}_2\text{O} \text{ (111)} + \text{CuO} \text{ (111)} + \text{Cu} \text{ (111)}]$ are displayed in Table S1. It can be observed

from Table S1 that the relative content of Cu₂O increases from 13 to 30.6 wt% with increasing reaction time from 0.5 to 4 hour when the Cu film is annealed at 350 °C. For the sample annealed at 450 °C, the peak intensity of Cu₂O along the (111) direction is the strongest with appreciable intensity of the (111) plane of CuO. At this temperature about 76.8 wt% of copper is oxidized to Cu₂O (61.6 wt%) and CuO (15.2 wt%). This is obtained as appropriate composition towards enhancing the photoelectrochemical performance of the system. As annealing temperature increase to 550 or 650 °C, the diffusion of oxygen into the films, oxidized the remaining Cu film and of Cu₂O into CuO phase. This is evident from XRD pattern that significantly diminished peak intensity of Cu film along (111) direction confirms the oxidation of Cu film into Cu₂O and subsequently CuO.

Table S1. Effects of annealing time and annealing temperature on phase composition

Annealing temp. (°C)	Annealing time (hr)	Wt _{Cu₂O} (%)	Wt _{CuO} (%)	Wt _{Cu} (%)
350	0.5	13.0	0	87.0
350	1.0	16.0	0	82.0
350	2.0	22.7	0	77.3
350	3.0	26.5	7.4	70.7
350	4.0	30.6	10.3	50.1
450	4.0	61.6	15.2	23.2
550	4.0	30.5	61.5	8.0
650	4.0	9.0	91.0	0

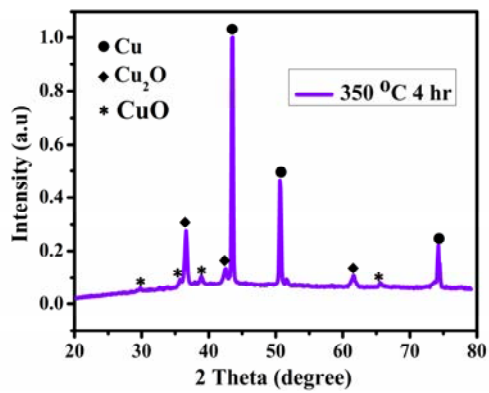


Figure S1 patterns of Cu film oxidized at 350 °C for 4 hr.

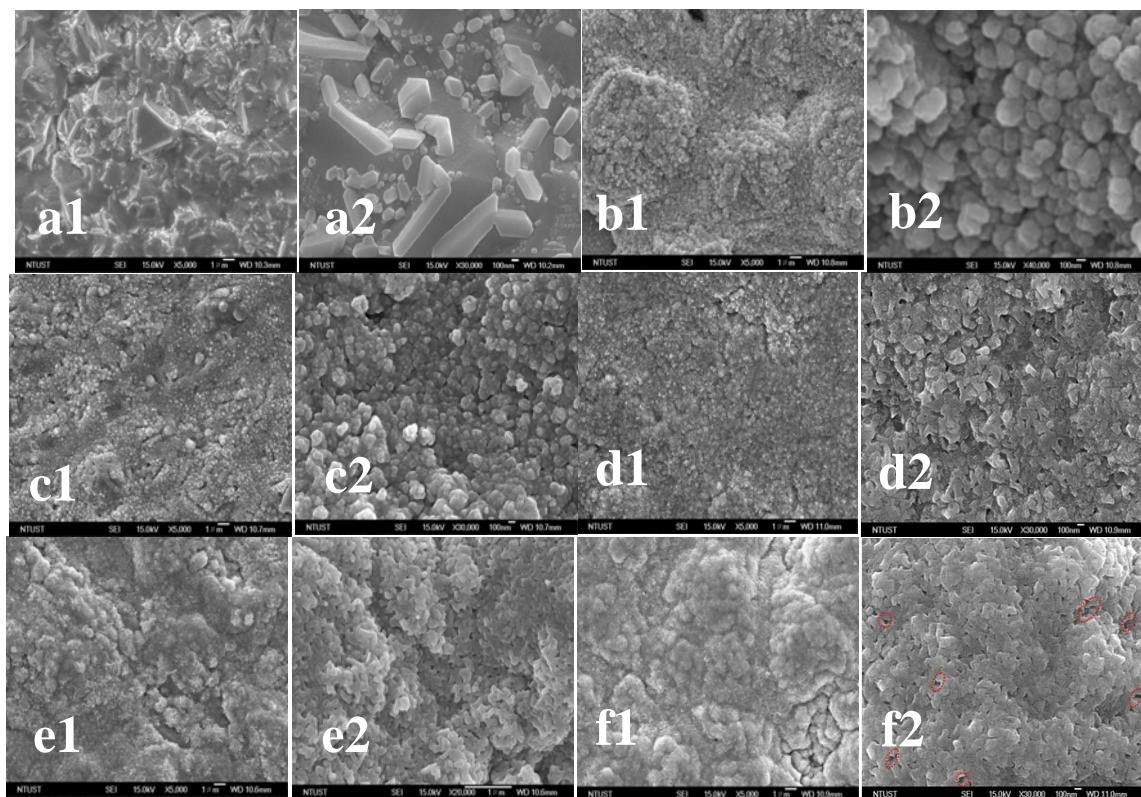


Figure S2. Scanning electron microscopy images of the as synthesized Cu film (a1-a2) and Cu film annealed at: 350 °C for 0.5 hr (b1-b2), 1 hr (c1-c2), 2 hr (d1-d2), 3 hr (e1-e2) and 4 hr (f1-f2).

Treatment temperature	Cu film	
(a) Before	Front Side	Back Side
(b) 350°C	Front Side	Back Side
(c) 450°C	Front Side	Back Side
(d) 550°C	Front Side	Back Side
(e) 650°C	Front Side	Back Side

Figure S3. Digital photographs of as-deposited Cu film and Cu films annealed at different temperatures: (a) Cu film deposited on FTO before thermal treatment, samples after 350°C (b), 450 °C (c), 550 °C (d) and 650 °C (e) thermal treatment.

To get further evidence about the surface roughness of the films, we performed Atomic force microscope (AFM) imaging of the films annealed at 350, 450, 550 and 650 °C. The two dimensional (5 μm x 5 μm) AFM images of Cu film before and after annealing were displayed in Figure S4. As shown in Figure S4c, Cu film annealed at 450 °C shows a higher roughness ($R_a = 122$ nm) than other annealed sample, which is in good agreement with the FE-SEM images. That is presumably due to the grain growth and densification of the film (Figure S4c) as a consequence of higher ionic mobility during annealing process, the surface roughness was increased from 90.2 nm to 122 nm when the annealing temperature was increased from 350 to 450 °C. The surface roughness decreases from 122 nm to 84.7 nm when the annealing temperature is increased from 450 to 550 °C due to the island coalescence which leads to a

smaller distance between the base and top of the islands. The Cu film annealed at 650 °C showed slightly rougher surface than film annealed at 550 °C. This is probably because of the formation of dislocations or pits in film annealed at 650 °C.

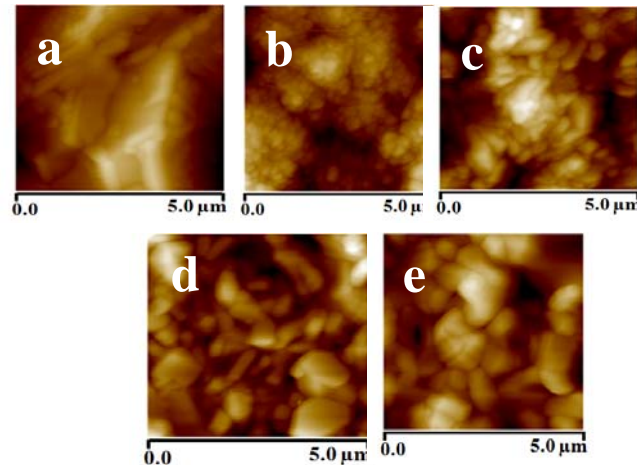
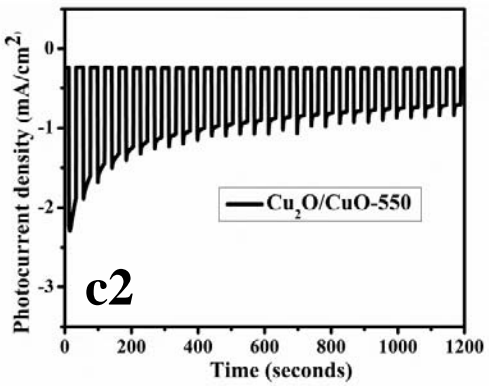
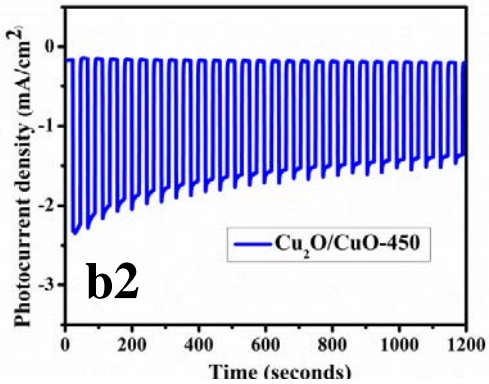
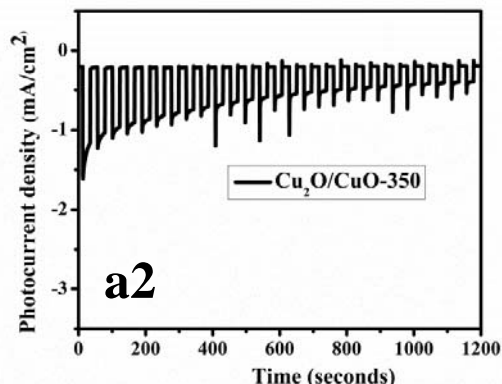
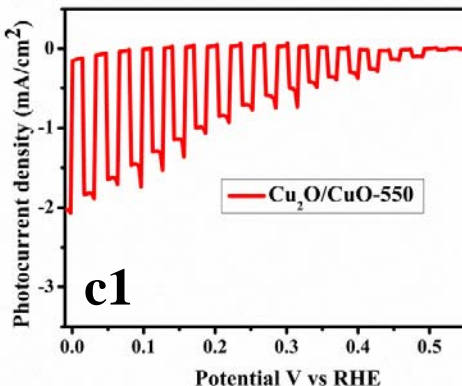
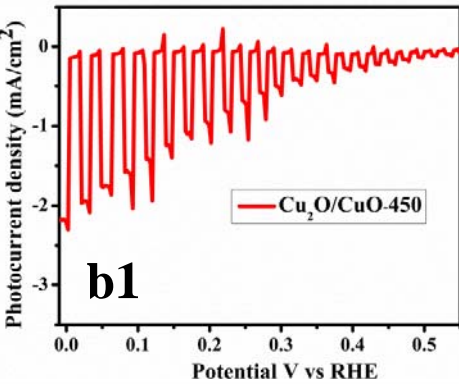
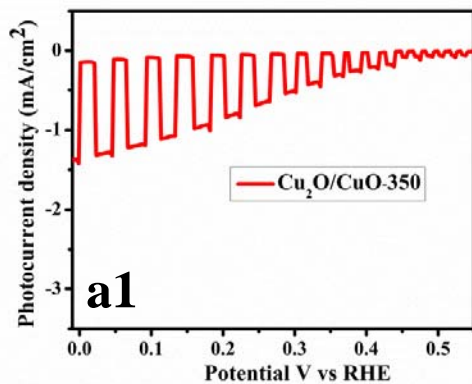


Figure S4. AFM images of as synthesized Cu film (a) and Cu film annealed at: 350 °C (b); 450 °C (c); 550 °C (d); 650 °C (e).

The relative photostability of Cu₂O/CuO-350, Cu₂O/CuO-450, Cu₂O/CuO-550 and Cu₂O/CuO-650 photocathodes (Figure S5a2, b2, c2, d2) were also examined by measuring the photocurrent density using chronoamperometric method at 0 V vs. RHE under chopped illumination. As shown in Figure S5, increasing annealing temperature enhances not only the photocurrent density but also the photostability of the photocathode, and the maximum photocurrent density (-2.1 mA/cm^2) was recorded with oxidation temperature of 450 °C (Cu₂O/CuO, Figure S5b2) at 0 V vs.RHE. On the other hand, the observed decrease in photocurrent density at lower annealing temperature (e.g. Cu₂O/CuO at 350 °C, Figure S5a2) is presumably due to the poor crystalline quality of the heterojunction. As shown in Figure S5c2 and d2, the photocathodes prepared at annealing temperature over 450 °C (Cu₂O/CuO-550 and Cu₂O/CuO-650) revealed maximum photocurrent density, -1.9 and -1.8 mA/cm^2 respectively, for the first few seconds rapidly decayed on the light on-off cycle for 20 minutes. The observed decrease in photocurrent density was due to the resulted higher CuO composition in the heterojunction, which is highly susceptible to undergo self reduction by the photogenerated charged particles.



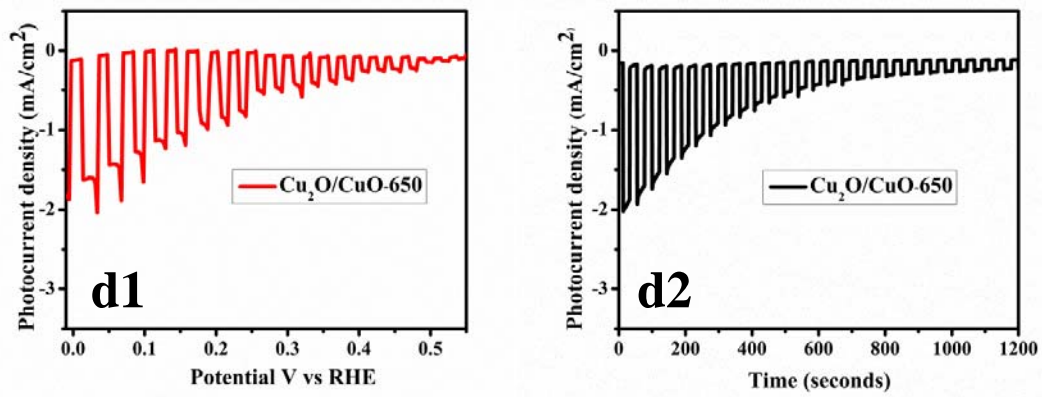
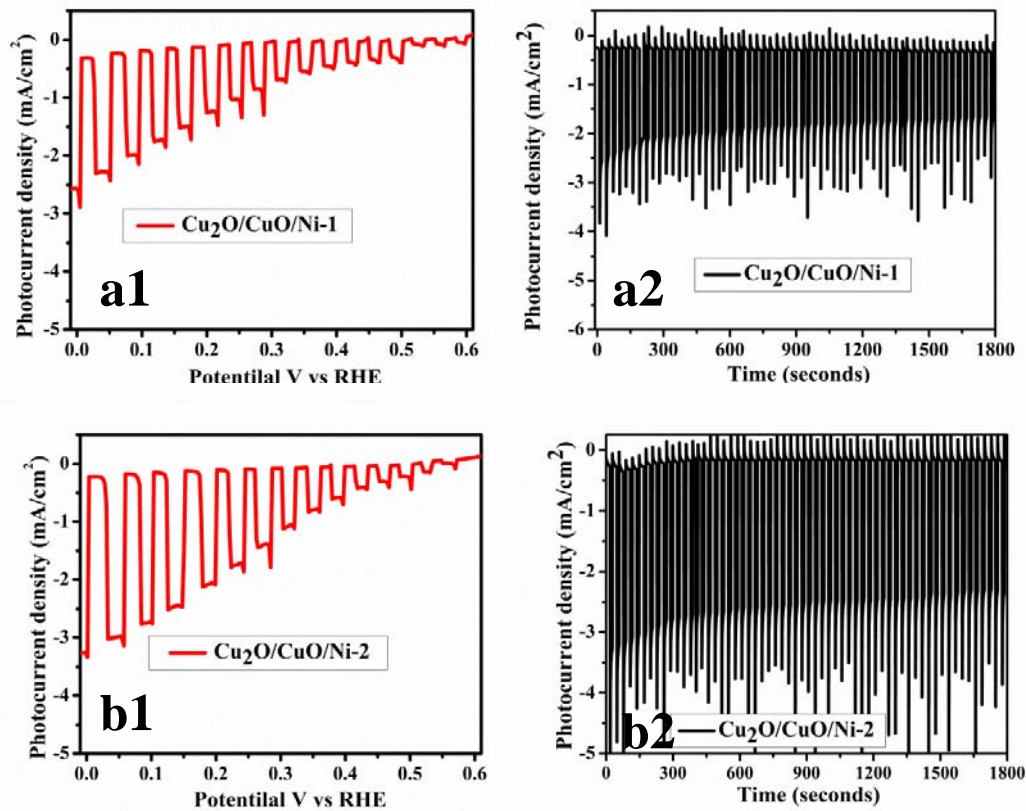


Figure S5. PEC performances and stability measurement of (a1, a2) $\text{Cu}_2\text{O}/\text{CuO-350}$, (b1, b2) $\text{Cu}_2\text{O}/\text{CuO-450}$, (c1, c2) $\text{Cu}_2\text{O}/\text{CuO-550}$ and (d1, d2) $\text{Cu}_2\text{O}/\text{CuO-650}$.



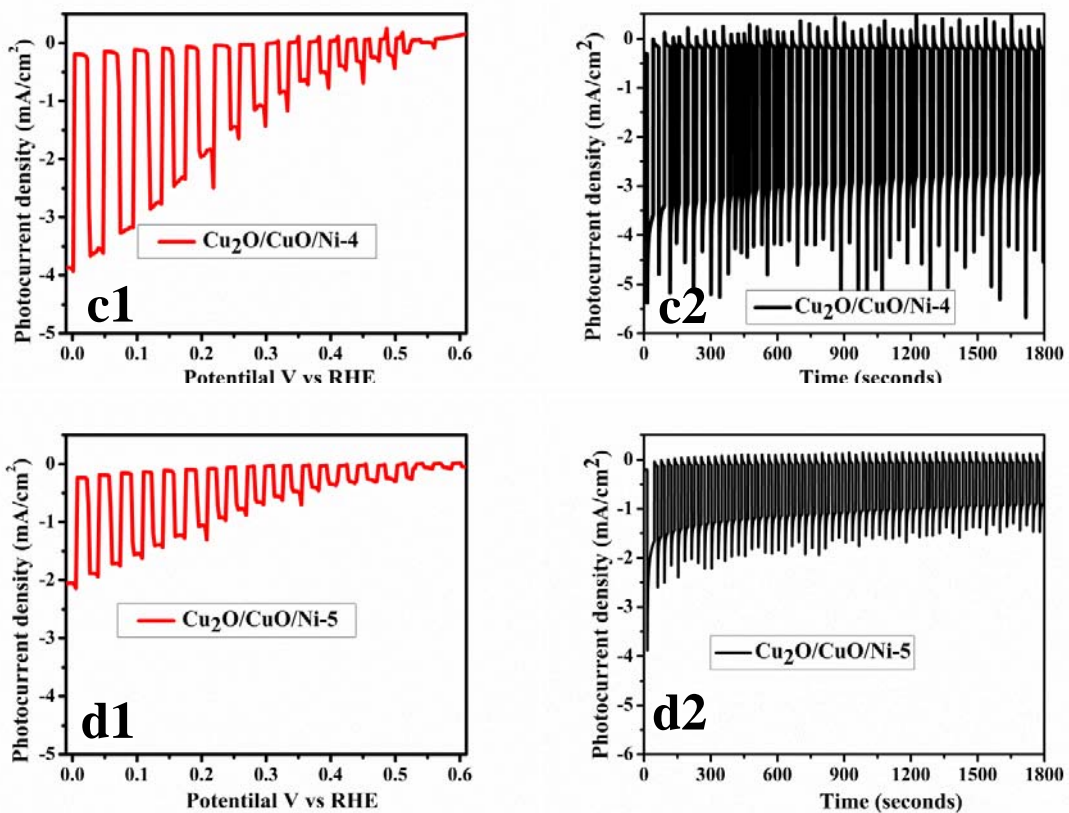


Figure S6. PEC performances and stability measurement of (a1, a2) $\text{Cu}_2\text{O}/\text{CuO}/\text{Ni}-1$; (b1, b2) $\text{Cu}_2\text{O}/\text{CuO}/\text{Ni}-2$; (c1, c2) $\text{Cu}_2\text{O}/\text{CuO}/\text{Ni}-4$ and (d1, d2) $\text{Cu}_2\text{O}/\text{CuO}/\text{Ni}-5$.

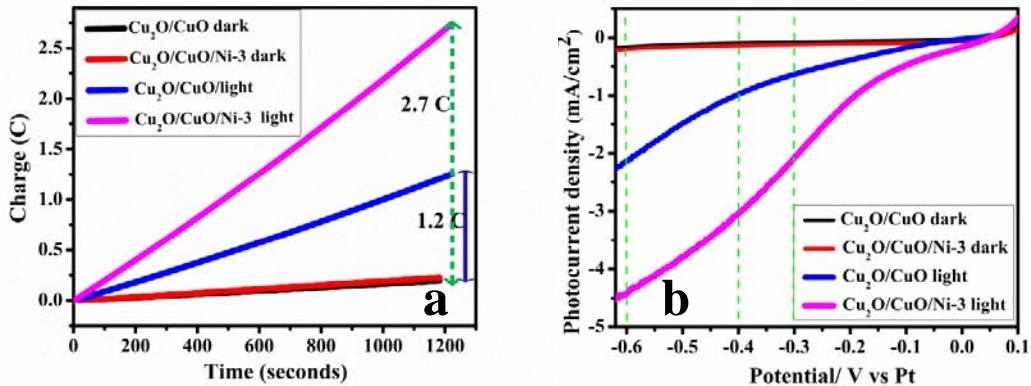


Figure S7. (a) Electrolysis response of Cu₂O/CuO and Cu₂O/CuO/Ni-3 photocathodes at an applied potential of 0 V vs. RHE under visible light illumination (blue and magenta colored curves) and dark (black and red colored curves) respectively. (b) Linear sweep voltammetry of Cu₂O/CuO and Cu₂O/CuO/Ni-3 in two electrode system under simulated one sun illumination (100 mW/cm²).

To gain characteristics features about the corrosion of the protective layer CuO, we further carried out XRD, XPS, XAS and EXAFS on bare Cu₂O/CuO and Cu₂O/CuO/Ni-3 photocathodes before and after the stability testing. Figure S8a and b shows the XRD results of bare Cu₂O/CuO and Cu₂O/CuO/Ni-3 before and after stability testing for 20 minutes respectively. Unlike the Cu₂O/CuO/Ni-3, the XRD pattern of the bare Cu₂O/CuO photocathode after stability testing revealed increase in reflections of the peaks corresponding to Cu₂O in the heterojunction. However, the XRD patterns of the Cu₂O/CuO/Ni-3 after stability test showed almost the same feature with its XRD patterns before stability test. This indicates that the Cu₂O/CuO photocathode decorated with nickel exhibits suppressed photoreduction of the protective layer and results in enhanced photostability of Cu₂O together with the presence of nickel cocatalyst.

To gain more insight into the chemical composition and extent of reduction of the protective layer (CuO) on the main light absorber (Cu₂O) of the Cu₂O/CuO photocathode, we also carried out XPS measurements on bare Cu₂O/CuO and Cu₂O/CuO/Ni-3 both before and after photostability test measurement for 20 minutes. The XPS survey spectra on Cu₂O/CuO/Ni-3 and

bare Cu₂O/CuO photocathodes shown in Figure S8c, revealed the presence of Cu, O and Ni elements and only Cu and O by the aforementioned photocathodes respectively. The core level spectrum of Ni 2p of the Cu₂O/CuO/Ni-3 photocathode was displayed in Figure S8d. Two main peaks located at 852.4 eV and at 870.7 eV, corresponding to Ni 2p_{3/2} and 2p_{1/2} respectively, can be assigned to an oxidation state of Ni⁰. This indicates that elemental nickel is perfectly deposited on the surface of Cu₂O/CuO.

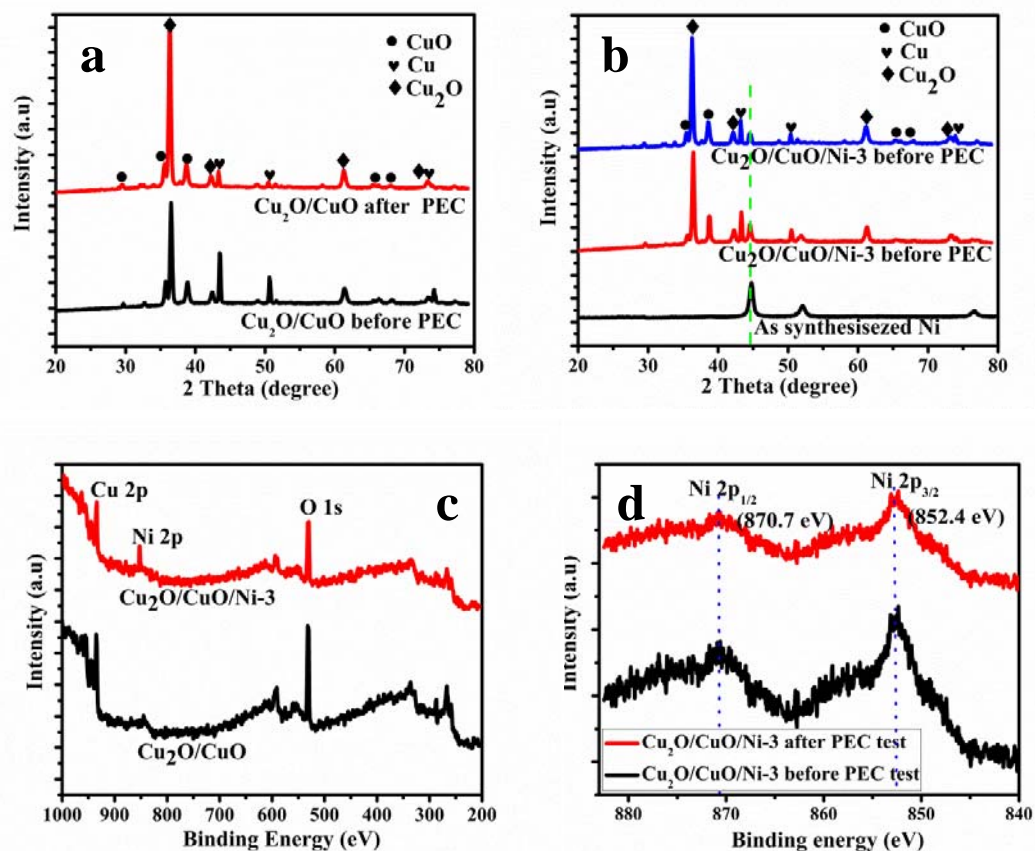


Figure S8. XRD patterns of Cu₂O/CuO (a) and Cu₂O/CuO/Ni-3 (b) before and after PEC test; XPS spectra of: (c) survey spectra of Cu₂O/CuO and Cu₂O/CuO/Ni-3 (d) Ni 2p core level of Cu₂O/CuO/Ni-3 before and after PEC test.

It is necessary to confirm whether the as synthesized nanoparticle is Ni or not and explore the distribution of Ni nanoparticles on the surface of the Cu₂O/CuO photocathode for the improvement of photocurrent density and photostability. Figure S9a shows the X-ray diffraction patterns for the as prepared Ni sample after reduction of NiCl₂.6H₂O for 10 hr using different amount of NaH₂PO₂ as reducing agent at 250 °C. The XRD patterns of the as synthesized Ni using 2.45 and 5.27 g of NaH₂PO₂ revealed different crystalline size but similar peaks at 44.6, 51.8 and 76.5° (red and black colored curves in Figure S9a). This indicates that the observed peaks are characteristics of face centered cubic (fcc) nickel phase without any apparent impurity peaks such as nickel oxide. The crystalline size of the nanoparticles was measured using Sherrer equation, and is found to be 24.3 nm and 11.8 nm for the particles synthesized using 2.45 and 5.27 g of NaH₂PO₂ as reductant respectively. On the other hand, when we further increased the amount of reductant, the as synthesized nanoparticles did not show up any characteristic peaks related with metallic nickel phase (blue and magenta colored curves in Figure S9a), indicating formation of some other compound than nickel. For our photoelectrochemical purpose we used the Ni nanoparticle synthesized using 5.27 g reductant. This is because small sized nanoparticles (cocatalyst) are efficient in enhancing the surface activation of the semiconductors. The XRD results here are in agreement with our XAS measurement in the later section. The SEM images of as synthesized Ni using 5.27 g reductant are shown in Figure S9b and S9c, where homogeneous and similar sized nanoparticles without agglomeration were revealed. In the present study, we also presented nickel nanoparticles synthesis using simple and environmentally friendly hydrothermal method. A possible effect of reaction conditions for synthesis of nickel nanoparticle will be addressed in later section.

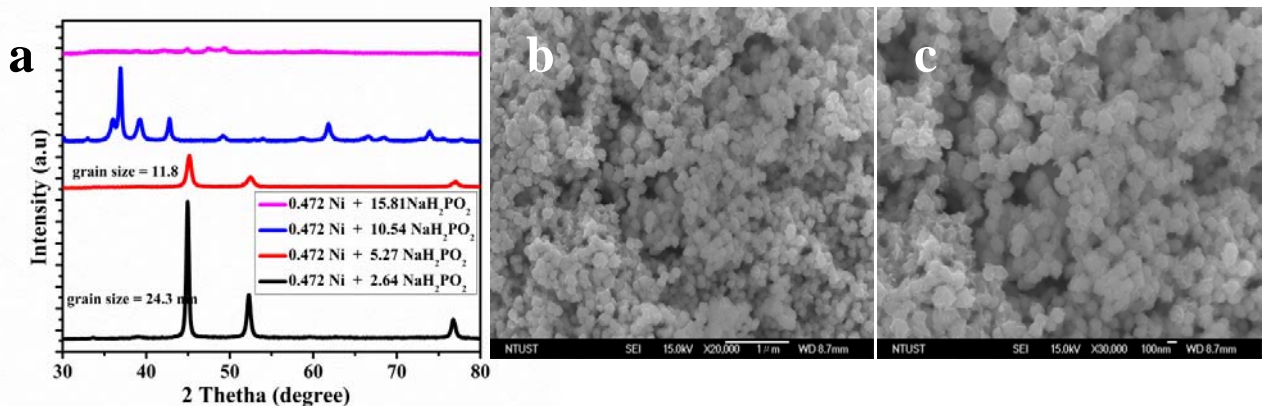


Figure S9. (a) XRD patterns of the product after reduction of $\text{NiCl}_2 \cdot 6\text{H}_2\text{O}$ for 10 hr at 250 °C using different amount of NaH_2PO_4 as reducing agent and (b and c) SEM images of as synthesized Ni.

The XRD patterns of bare $\text{Cu}_2\text{O}/\text{CuO}$ and nickel decorated $\text{Cu}_2\text{O}/\text{CuO}$ heterojunction are displayed in Figure S10a. At lower amount of Ni deposition there is no emerging new peak corresponding to Ni. Meanwhile, at higher amount of Ni deposition, a weak peak appeared at about 44.7° suggests the effective deposition of Ni. It is interesting that the SEM image displayed in Figure S10b showed uniformly deposited Ni nanoparticles on the surface of $\text{Cu}_2\text{O}/\text{CuO}$ photocathodes. The presence of Ni on the surface of $\text{Cu}_2\text{O}/\text{CuO}$ was further strengthen by EDX analysis given in Figure S10c. This facile deposition by spin coating gives a straightforward and adaptable strategy for depositing optimum amount of Ni cocatalyst on the surface, evading development of islands and knobs altogether, and such a uniform deposition would bring about enhanced $\text{Cu}_2\text{O}/\text{CuO}/\text{Ni}$ PEC performance.

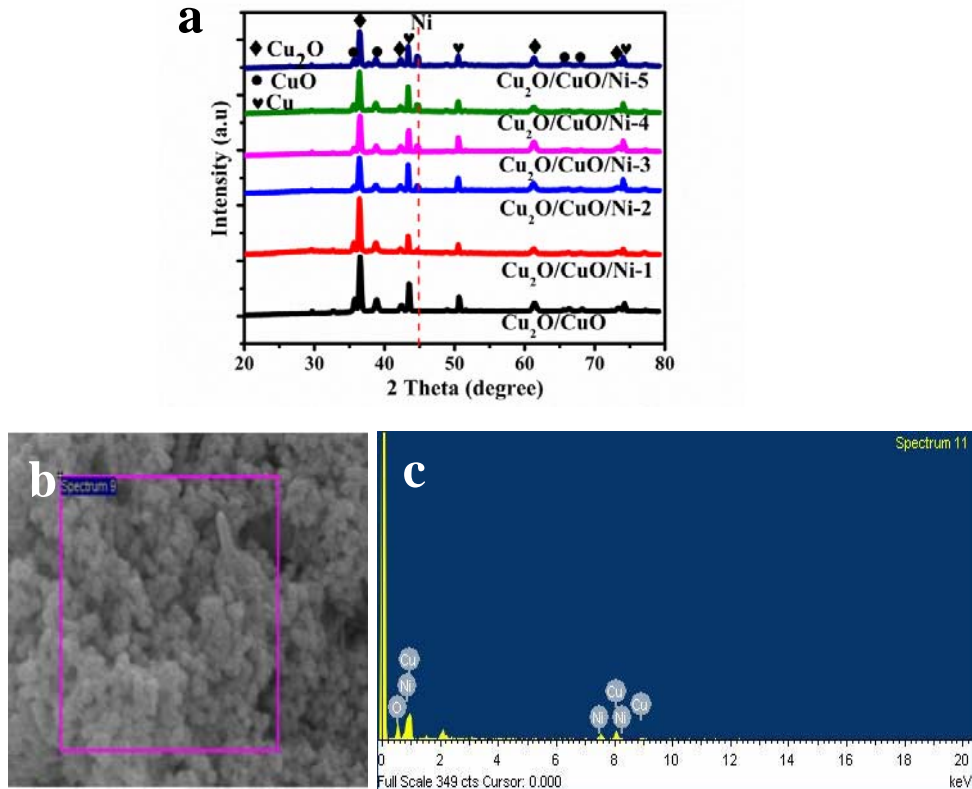


Figure S10. (a) XRD pattern of the Cu₂O/CuO and Cu₂O/CuO/Ni-x (b) SEM image for EDX analysis (c) Typical EDX analysis acquired from the Cu₂O/CuO/Ni-3 photocathode film. It can be seen that a weak Ni peak was detected together with Cu and O.

To further assure the effective synthesis and deposition of Ni, we carried out Ni-K-edge XANES and EXAFS studies on the as synthesized Ni and Cu₂O/CuO/Ni-3 heterojunction both before and after PEC test. For comparison, the XANES spectra of Ni foil and NiO as a reference, representing Ni⁰ and Ni²⁺ state respectively, were displayed in Figure S11a together with XANES spectra of as synthesized Ni and Ni on Cu₂O/CuO/Ni-3. As shown in Figure S11b, the edge position of the as synthesized Ni is slightly shifted to the higher energy values, implying the oxidation state of as synthesized Ni is slightly higher than that of the Ni foil. This is reasonable because the surface oxidation is happened due to the nanoscale. The XANES spectral feature of Ni on the sample before PEC test is similar to that of the as synthesized Ni, only the energy is just a little bit higher. This is presumably due to the Ni is deposited on the Cu₂O/CuO and charge balance is taken place. As clearly shown in Figure S11b, the Ni K-edge of the Cu₂O/CuO/Ni-3

photoelectrode after PEC is slightly shifted to the lower energy values, indicating Ni is reduced a little bit. We inferred that when the Cu₂O/CuO without Ni during PEC operation, the rate of electron injected to electrolyte is slow and the charge balance would be taken place on Cu species. However, the oxidation state of Cu is reduced. On the other side, when the Cu₂O/CuO with Ni during the PEC operation, the reduction of Ni is generation first due to the surface oxygen of Ni would be removed at the initial state, and then the rate of electron injected to electrolyte is increased after reduction. Besides, a slightly decrease in peak intensity of the photocathode after PEC test (black colored curve in Figure S11b), is probably due to the detachment of the outmost Ni from the Cu₂O/CuO surface. The Fourier transformed (FT) magnitudes of the as synthesized Ni and Cu₂O/CuO/Ni-3 and their κ^2 - weighted spectra are displayed in Figure S11c and S11d respectively. One can easily observe that data before and after PEC test are very similar, revealing the presence of one main peak at 2.2 Å (Figure S11c), which corresponds to the Ni-Ni bonds. The similarity in Ni-K-edge EXAFS before and after PEC test is probably due to the local environment of Ni atoms is much the same in both samples. Besides, the absence of the Ni-O bonds both before and after PEC test indicates the high stability of deposited Ni.

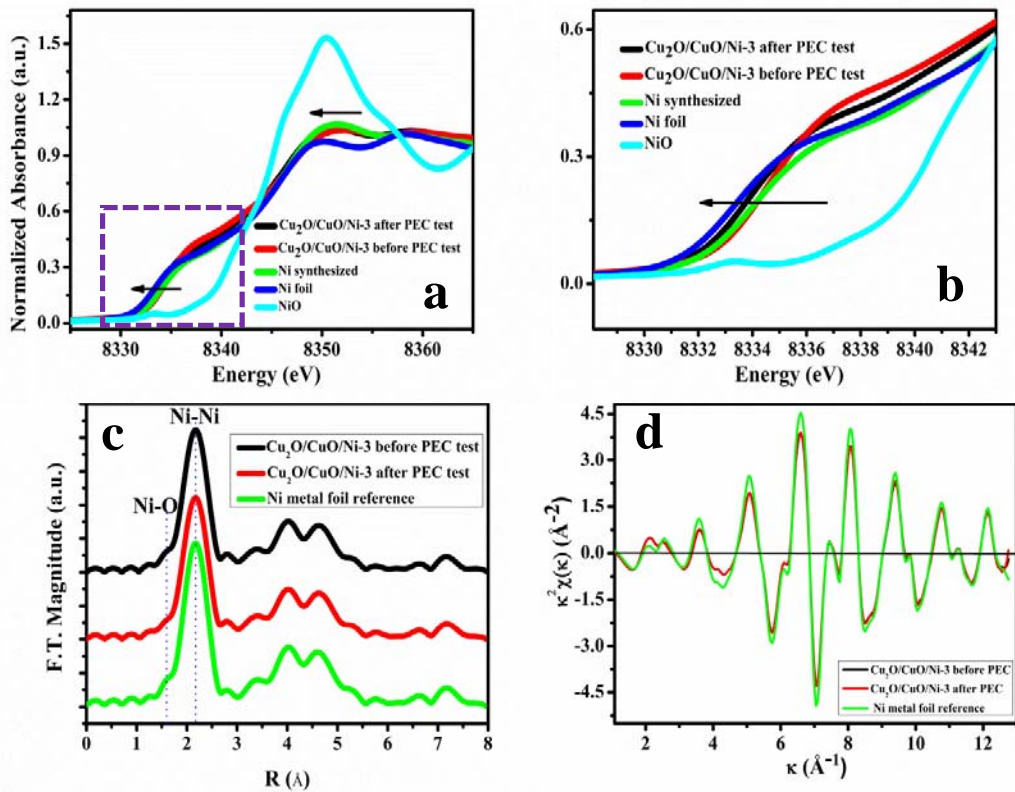


Figure S11. (a) Ni-K-edge XANES spectra of Ni foil (blue colored curve), as synthesized Ni (green colored) and $\text{Cu}_2\text{O}/\text{CuO}/\text{Ni-3}$ both before and after PEC test (b) enlargement of selected portion of curve a and (c, d) Ni-K-edge EXAFS spectra of $\text{Cu}_2\text{O}/\text{CuO}/\text{Ni-3}$ both before and after PEC test in r and κ - space respectively.

Once we confirmed the formation of Cu_2O and CuO in the bulk and on the surface respectively, we measured cross-sectional SEM image of $\text{Cu}_2\text{O}/\text{CuO}/\text{Ni-3}$ photoelectrode to roughly determine the thickness of the Cu_2O and CuO layers. Figure S12 is a cross-sectional SEM image of $\text{Cu}_2\text{O}/\text{CuO}/\text{Ni-3}$ sample, from which a three-layered structure can be identified: a 6 μm thick bottom layer that lies directly above the FTO substrate, an intermediate thin layer with a thickness of about 2 μm , and a top nickel cocatalyst layer.

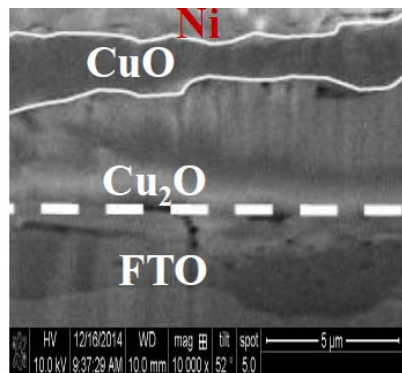


Figure S12. Cross section SEM images of Cu₂O/CuO/Ni-3

To provide further evidence about our suggestion, the detachment of Ni into the electrolyte solution after PEC test, we performed Ni quantification using ICP-AES both in pure electrolyte before PEC, in the residue of the electrolyte taken after PEC test and etched and digested Cu₂O/CuO/Ni-3 film from the FTO substrate after PEC test for comparison. As shown in Table S2, small amount of Ni was quantified in the residue of the electrolyte after PEC test (0.5 ppb), indicating slight detachment of outmost Ni from the Cu₂O/CuO/Ni-3 surface during PEC test. This is concluded because Ni was not detected at all in the pure electrolyte before PEC test. The large amount of Ni quantified in the digested Cu₂O/CuO/Ni-3 sample after PEC test further confirms the effective deposition of Ni.

Figure S13 shows ICP-AES five point Ni calibration curve with quite good correlation coefficient $r^2 = 0.9999$ was obtained by measuring concentration of standard solutions prepared from stock standard (1000 ppm) by dilution. The samples whose Ni content needs to be investigated were prepared as follows: The Cu₂O/CuO/Ni-3 heterojunction after PEC test for 20 minutes was etched and digested in aqua regia (4.5 ml HCl and 1.5 ml HNO₃). The sample was ultrasonicated for 10 minutes at room temperature before heating on a hot plate at 70 °C for 60 minutes. After cooling, the samples were filtered and diluted to 20 ml in a polyethylene flask. The filtrate was filtered again with syringe needle filter. The sample from the residue of the electrolyte after PEC test was prepared with ultrasonication followed by heat treatment on a hot plate for 60 minute. This procedure was done to enhance the solubility of any detached outmost

Ni after PEC test in the electrolyte. The sample from the electrolyte before PEC test was directly introduced for analysis without further special treatment. Ni quantification in all the samples and standard solutions were done using a JY200-2 ICP-AES instrument. As expected, Ni was not detected in the fresh electrolyte before PEC test whilst a very negligible (0.5 ppb) amount of Ni was detected in the residue of the electrolyte solution taken after PEC test. A low amount of Ni detection in the residue of the electrolyte after PEC test confirms relatively a good adhesion of Ni with the photocathode material.

Table S2 ICP-AES data

Sample	Conc.
Pure electrolyte before PEC test	0
Residue in electrolyte after PEC test	0.05 ppb
Cu ₂ O/CuO/Ni-3 heterojunction after PEC test	40.7 ppm

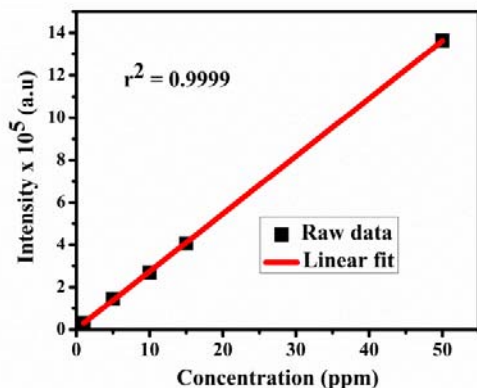


Figure S13. ICP-AES five point Ni calibration curve

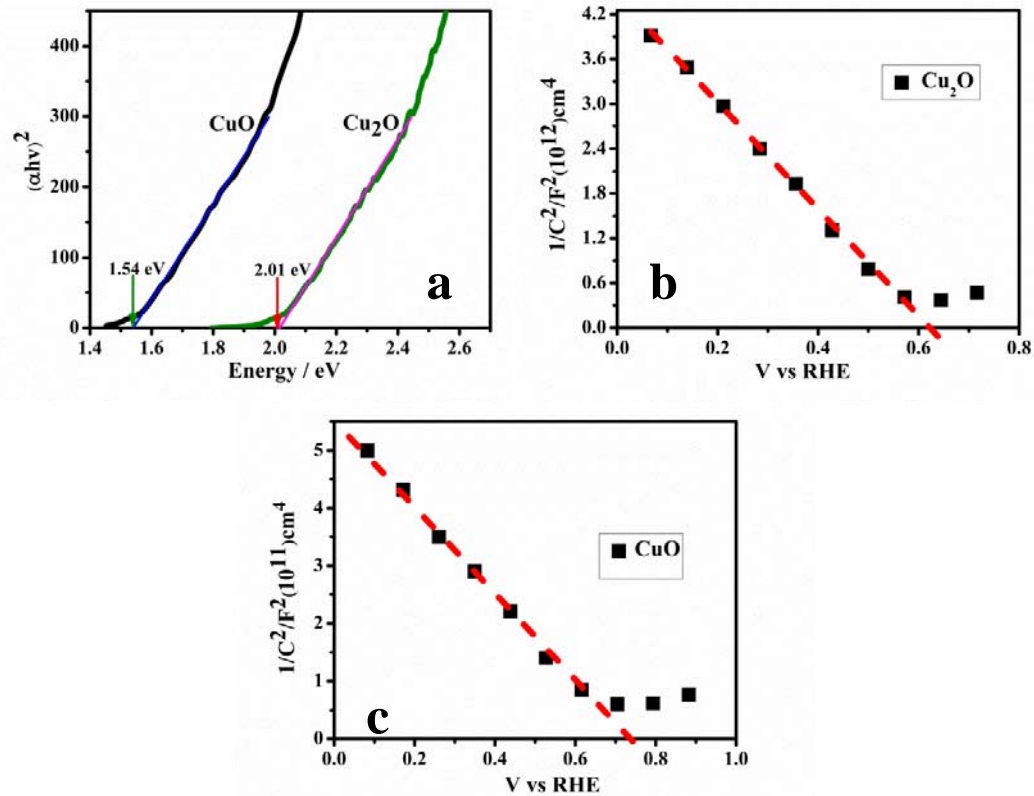


Figure S14 (a) Tauc plot of Cu_2O and CuO; (b) and (c) Mott–Schottky plot of Cu_2O and CuO in 1.0 M Na_2SO_4 electrolyte (pH 5) respectively.

1. Hu, L.; Huang, Y.; Zhang, F.; Chen, Q. CuO/ Cu_2O composite hollow polyhedrons fabricated from metal-organic framework templates for lithium-ion battery anodes with a long cycling life. *Nanoscale* 2013, 5, 4186-4190.